Scientific paper

Synthesis, Crystal Structures, and Antibacterial Evaluation of Metal Complexes Based on Functionalized 2-phenylquinoline Derivatives

Jie Qin,[1]*,[2] Fu-Xiang Li,[1] Le Xue,[1] Na Lei,[1] Qing-Ling Ren,[1] Dan-Yang Wang[1] and Hai-Liang Zhu[1]

[1] *School of Life Sciences, Shandong University of Technology, Zibo, China*

[2] *State Key Laboratory of Coordination Chemistry, School of Chemistry and Chemical Engineering, Nanjing University, Nanjing, China*

* *Corresponding author: E-mail: qinjietutu@163.com*

Received: 17-12-2013

Abstract

A series of dinuclear paddle-wheel like transition metal complexes based on 2-phenylquinoline-4-carboxylic derivative **L** have been synthesized and characterized by IR, elemental analysis, and X-ray diffraction single crystal analysis. The biological activities of **L** and its complexes were evaluated as assayed antibacterial activities, including *Escherichia coli, Pseudomonas aeruginosa*, *Bacillus subtilis* and *Staphylococcus aureus*. The results indicated that these complexes showed better antibacterial activities than the free ligand or metal salts alone. Among them, the Zn(II) and Cd(II) complexes with IC_{50} of 0.57 μg/mL and 0.51 μg/mL, respectively, showed excellent antibacterial activity against *Staphylococcus aureus*.

Keywords: Quinoline derivative; Metal complex; X-ray crystal structure; Antibacterial activity.

1. Introduction

Since the successful use of cisplatin and related platinum complexes as anticancer agents, developing biologically active metal complexes as potential therapeutic agents has become a central research theme in bioinorganic chemistry.[1–5] These metal complexes could act *via* dual or multiple mechanisms of action by combining the pharmacological properties of both the ligand and the metal ion.[6] Moreover, depending on the coordination effect, metal centers are able to organize the ligands to achieve pharmacophore geometries which are not available for the organic drug molecules.[7,8] Based on the above consideration, exploration of metal-based compounds is an attractive approach to obtain novel antibacterial drug candidates,[8,9] as multidrug-resistant bacteria have become a serious medical problem.[10]

Compounds containing quinoline moiety have received special attention in chemical, medicinal and pharmaceutical research, as this structural scaffold is found in a variety of drugs. For example, 8-hydroxyquinoline (8HQ) has been used as a fungicide in agriculture.[11] Meanwhile, 8HQ is capable of forming complexes with divalent metal ions through chelation, which is useful for the treatment of metal-related diseases.[12] Owing to the excellent clinical effcacy, low toxicity, and cheap synthesis, the 4-aminoquinoline class of therapeutics remains a frontline drug of choice for combating malaria.[13] Platinum(II) complexes derived from 4-amino-7-chloroquinoline derivatives presented promising results against *Mycobacterium tuberculosis*.[14] Some antibacterial drugs containing quinolone skeleton, when administered as metal complexes showed increased activity as compared to the ligand involved.[9, 15]

Carboxylic derivatives are useful building blocks for the construction of metal-organic frameworks, due to their strong coordination ability and diverse coordination modes.[16,17] Meanwhile, they are endowed with hydrogen-bonding capabilities to prepare intriguing supramolecular systems. Carboxylic derivatives are also suggested to have broad biological activity. For example, Pruchnik *et al*. have reported that tributyltin aminoarylcarboxylates can be used as cytostatic agent.[18] Some salicylic acid derivatives,

such as anacardic acids, salicylhydroxamic acids, and metronidazole modified salicylic acid derivatives were reported as urease inhibitors.[19–21] The reaction of tetrafluorophthalic acid with $AgNO_3$ produced light-stable and water-soluble Ag(I) coordination polymers, which exhibited significantly higher effective antibacterial activity than tetrafluorophthalic acid.[22] Zinc complex derived from oxolinic acid and $ZnCl_2$ showed high bonding ability to calf-thymus DNA (CT DNA).[23]

Therefore we are focusing on designing and synthesizing carboxyl modified quinoline derivatives. In the present work, 2-(4-bromophenyl)quinoline-4-carboxylic acid (**L**) (Scheme 1) has been synthesized in high yields and fully characterized by IR, ^{1}H NMR, and elemental analysis. Further coordination reactions of the ligand with metal acetates afford dinuclear paddle-wheel complexes with the general formular $M_2(L)_4(CH_3OH)_4$ (M = Mn^{II}, **1**; M = Co^{II}, **2**; M = Zn^{II}, **3**; M = Cd^{II}, **4**). Herein, we describe the preparation, characterization, and the crystallographic analyses of the novel complexes. The antibacterial activity of the free ligand **L** and its metal complexes **1**–**4** was evaluated on *Escherichia coli* ATCC 35218, *Pseudomonas aeruginosa* ATCC 27853, *Bacillus subtilis* ATCC 6633 and *Staphylococcus aureus* ATCC 6538.

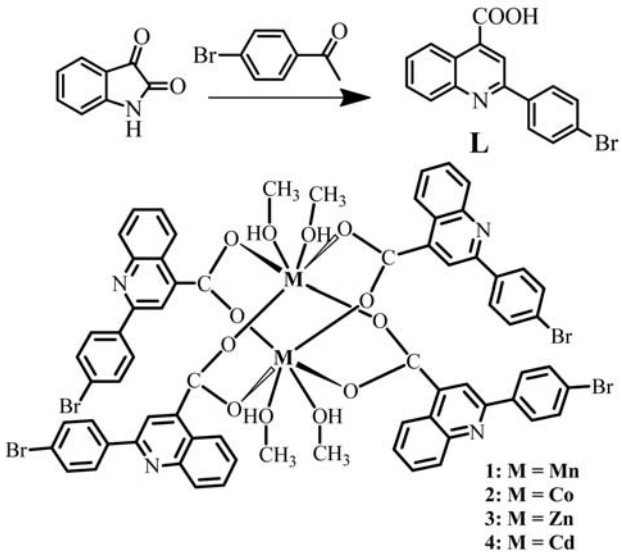

Scheme 1. Synthetic Routes to Ligand **L** and Complexes **1**–**4**.

2. Results and Discussion

2. 1. Synthesis and Characterization

The synthetic pathway is outlined in Scheme 1. The quinoline carboxylic ligand **L** was prepared *via* the Pfitzinger reaction starting from isatin and bromine-substituted acetophenone in high yield.[24] **L** is stable and can dissolve in polar solvents such as methanol and dimethyl sulfoxide (DMSO). In IR spectra, the typical stretching band ν(C=O) of carboxylic group for **L** is observed at 1714 cm^{-1}.

Reactions of manganese acetate, cobalt acetate, zinc acetate and cadmium acetate with one molar equivalent of **L** in methanol solution at room temperature afforded the corresponding complexes **1**–**4** in satisfactory yields. All the complexes are air-stable, the characterizations were carried out with their crystal samples. The IR spectra of these compounds are similar. They all show broad band ranging from 3446 cm^{-1} to 3060 cm^{-1}, indicating the O–H stretching of the methanol molecules. The asymmetric stretching mode ν_{as}(COO$^-$) is located around 1588 cm^{-1}, while the strong symmetric stretching mode ν_s(COO$^-$) for complex **1**–**4** is clearly visible around 1403 cm^{-1}. Therefo-

Table 1. Crystallographic data for **1**–**4**.

	1	**2**	**3**	**4**
empirical formula	$C_{68}H_{52}Br_4N_4O_{12}Mn_2$	$C_{68}H_{52}Br_4N_4O_{12}Co_2$	$C_{68}H_{52}Br_4N_4O_{12}Zn_2$	$C_{68}H_{52}Br_4N_4O_{12}Cd_2$
M_r	1546.66	1554.64	1567.52	1661.58
cryst syst	tetragonal	tetragonal	tetragonal	tetragonal
Space group	*I*4(1)/a	*I*4(1)/a	*I*4(1)/a	*I*4(1)/a
a (Å)	22.0434(8)	21.9272(6)	21.9395(5)	22.2704(4)
b (Å)	22.0434(8)	21.9272(6)	21.9395(5)	22.2704(4)
c (Å)	12.4887(9)	12.4881(7)	12.5238(6)	12.4016(5)
$\alpha = b = g$ (°)	90.00	90.00	90.00	90.00
V (Å^3)	6068.4(5)	6004.3(4)	6028.2(3)	6150.8(3)
Z	4	4	4	4
ρc (g cm^{-3})	1.693	1.720	1.727	1.794
F(000)	3096	3112	695	3280
T / K	293(2)	293(2)	293(2)	293(2)
μ(Mo-Kα)/ mm^{-1}	3.119	3.285	3.517	3.358
Data / param. / restr.	2706 / 205 / 0	2656 / 206 / 0	2877 / 205 / 0	3163 / 208 / 1
GOF	1.036	1.015	1.026	1.062
R_1, wR_2 ($I > 2\sigma(I)$)	0.0349 / 0.0802	0.0346 / 0.0700	0.0319 / 0.0664	0.0265 / 0.0585
R_1, wR_2 (all data)	0.0531 / 0.0885	0.0581 /0.0784	0.0542 / 0.0749	0.0354 / 0.0627
Large diff. peak / hole (e Å^{-3})	0.585 / –0.530	0.551 / –0.433	0.783 / –0.353	0.760 / –0.545

Table 2. Selected Bond Distance (Å) and Angles (deg) for **4**.

Cd(1)-O(1)$^{\#2}$	2.3382(8)	Cd(1)-O(2)	2.2208(8)
Cd(1)-O(3)	2.3242(9)	Br(1)-C(3)	1.898(3)
C(16)-O(1)	1.236(3)	C(16)-O(2)	1.256(3)
O(2)$^{\#1}$-Cd(1)-O(2)	169.58(1)	O(2)$^{\#1}$-Cd(1)-O(3)	85.75(7)
O(2)-Cd(1)-O(3)	102.42(7)	O(3)-Cd(1)-O(3)$^{\#1}$	78.26(1)
O(2)$^{\#1}$-Cd(1)-O(1)$^{\#2}$	92.05(7)	O(2)-Cd(1)-O(1)$^{\#2}$	83.23(8)
O(3)-Cd(1)-O(1)$^{\#2}$	79.41(7)	O(3)$^{\#1}$-Cd(1)-O(1)$^{\#2}$	152.29(7)
O(1)$^{\#2}$-Cd(1)-O(1)$^{\#3}$	126.23(1)	O(1)-C(16)-O(2)	127.5(2)

Symmetry transformations used to generate equivalent atoms:
#1 $-x+1, -y+1/2, z$; #2 $-y+3/4, x-1/4, -z-1/4$; #3 $y+1/4, -x+3/4, -z-1/4$

re, the $\Delta\nu$ values [$\nu_{as}(COO^-) - \nu_s(COO^-)$] of about 185 cm^{-1} are in good agreement with their bridging bidentate coordination mode features shown by the results of crystal structures.[17] The absorption spectra of reported compounds were measured in DMSO/H_2O (1:1) solution at room temperature (Figure S1).

The solid structures of complexes **1**–**4** were determined by single-crystal X-ray diffraction. The crystallographic and data collection parameters are given in Table 1; selected bond lengths and angles are listed in Tables 2 and S1–S3.

Single-crystal analysis indicates that complexes **1**–**4** are isostructual. They all crystallize in tetragonal space group $I4_1/a$. Here we describe only **4** in detail. The ORTEP plots of **1**–**4** with the atomic numbering scheme are shown in Figures S2–S4 and 1.

The structure of **4** consists of a centrosymmetric wheel-shaped dinuclear neutral molecule [$Cd_2(L)_4(MeOH)_4$], where two crystallographically identical Cd^{II} centers bridged by four **L** ligands (Figure 1). Most of the paddle wheel carboxylate complexes found in CCDC have a coordination number 5, while for complexes **1**–**4**, two methanol molecules are coordinated to one metal center to achieve the coordination number 6. In complex **4**, each Cd^{2+} adopts a distorted octahedral geometry formed by two oxygen atoms from methanol molecules and two atoms from carboxyl in the equal plane. The axial Cd1–O2 bond distance of 2.2208 Å is the shortest among the all Cd–O bonds. In the dinuclear unit, the Cd···Cd distance is 3.4819 (4) Å, which is within the normal range observed for the structures of Cd^{II} carboxylate complexes.[25, 26]

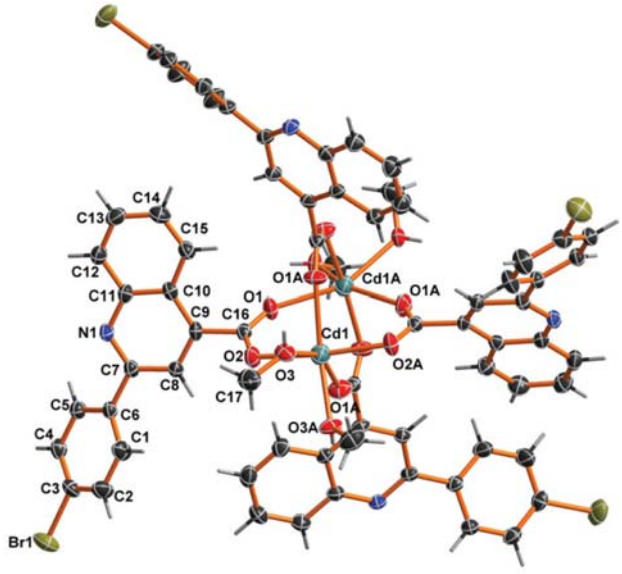

Figure 1. ORTEP view of **4** at the 50% probability level.

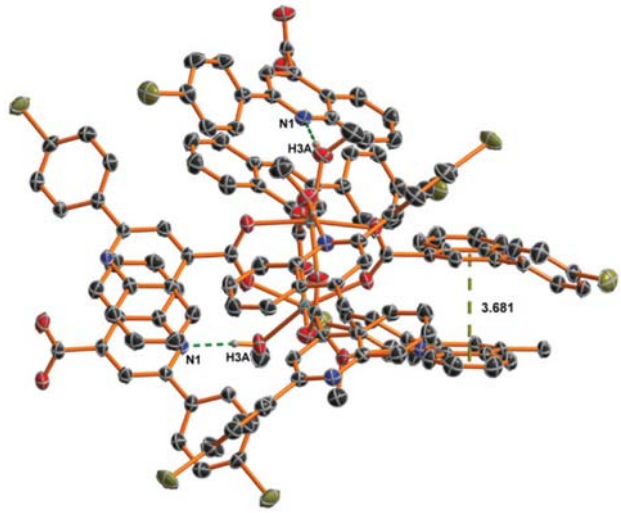

Figure 2. The non-bonding interactions in complex **4**.

The carboxylate group of **L** in complex **4** adopts a *syn-syn* bidentate bridging coordination mode, while the nitrogen atom doesn't participate in coordination. The ligand **L** is twisted in complex **4**, the dihedral angle between the substituted benzene ring (C(1)-C(6)) and quinoline ring is 34.75(7)°, and the dihedral angle between the carboxylate plane and the quinoline group is 66.21(2)°. It should be noted that complex **4** is stabilized by intermolecular O–H···N hydrogen bonding interactions. Each uncoordinated N(1) atom of the quinoline group serves as an acceptor to form intermolecular

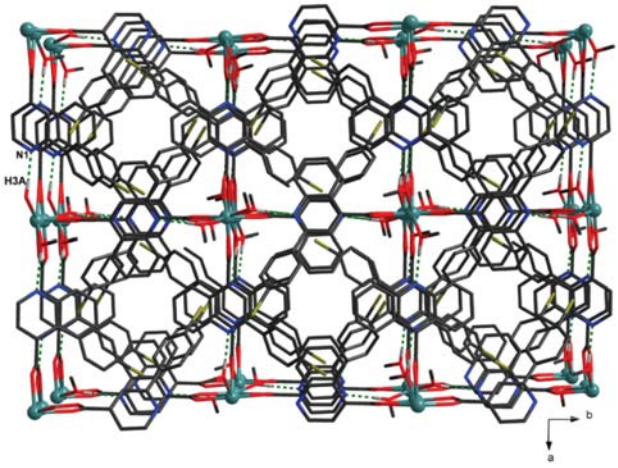

Figure 3. A perspective view of the hydrogen-bonded-driven 3D network of **4**.

hydrogen bonds with the coordinated methanol molecule (O3–H3A···N1, H3A to N1 distance 1.803(2) Å, O3–H3A···N1 angle 174(5)°, symmetry code: y + 1/4, $–x$ + 5/4, z + 1/4) (Figure 2), eventually forming the three dimensional network of **4** (Figure 3). Meanwhile, the adjacent quinoline rings from different dinuclear units are approximately parallel to each other (the dihedral angle is 2.669(7)°) with a centroid-centroid distance of 3.681(1) Å, indicating the presence of face-to-face π···π stacking interactions (Figure 2).

2. 2. In vitro Antibacterial Assay

The antibacterial activity was performed against two Gram-negative bacterial strains: *E. coli* and *P. aeruginosa* and two Gram-positive bacterial strains: *B. subtilis* and *S. aureus* by 3-(4,5-dimethylthia-zol-2-yl)-2,5-diphenyltetrazolium bromide (MTT) method. Clinically used antibiotics streptomycin, penicillin and ciprofloxacin were used as reference. The effectivity of the complexes **1**–**4** was evaluated in comparison to the free ligand **L** and the parent metal acetates. The half maximal inhibitory concentrations (HMICs) of the compounds against these bacteria were presented in Table 3.

As shown in Table 3, though no obvious antibacterial effect of the free ligand nor the metal salts alone were found against the tested bacteria, most of quinoline metal complexes exhibited (see below) antibacterial activity. Complex **1** showed moderate activity against *B. subtilis* with HMIC values of 7.30 *u*M. Complex **2** had a broad antibacterial spectrum against *S. aureus* and *E. coli* (HMIC = 6.61 and 5.10 *u*M, respectively) which was comparable to the positive control streptomycin. While, complexes **3** and **4** exhibited potent antibacterial activities against *B. subtilis* (HMIC = 1.48 and 1.59 *u*M, respectively) and *S. aureus* (HMIC = 0.36 and 0.31 *u*M, respectively), which were more effective than the streptomycin and penicillin. but they were completely inactive against *E. coli* and *P. aeruginosa*. Compared with ciprofloxacin containing quinolone skeleton, complexes **1**–**4** showed almost no activities against Gram-negative bacterial strains, except complex **2** showed moderate activity against *E. coli*. With regard to the Gram-positive bacterial strains: *B. subtilis* and *S. aureus*, ciprofloxacin also showed higher activities than complexes **1**–**4**.

The above results suggested that these carboxylic complexes possess broad and effective antibacterial activity. The biological activities of these complexes may be related to their structure presenting a more effective "lipophilic package". According to the X-ray structural analysis, each complex has four replaceable CH_3OH molecules and hence can coordinate with biomolecules, leading to the enhanced antibacterial activity.[16,26] We concluded that the structure factors which govern antimicrobial activities are strongly dependent on the central metal ion.

Table 3. Antimicrobial activity of the tested compounds.

Compounds	Half maximal inhibitory concentrations *(u*M*)*			
	Gram-positive		Gram-negative	
	B.subtilis	***S.aureus***	***E.coli***	***P.aeruginosa***
1	7.30	>100	>100	>100
2	>100	6.61	5.10	>100
3	1.48	0.36	>100	>100
4	1.59	0.31	>100	>100
L	>100	>100	>100	>100
$Mn(OAC)_2$	>100	>100	>100	>100
$Co(OAC)_2$	>100	>100	>100	>100
$Zn(OAC)_2$	>100	>100	>100	>100
$Cd(OAC)_2$	>100	>100	>100	>100
Streptomycin	2.35	3.17	2.61	>100
Penicillin	2.33	0.73	17.56	17.56
Ciprofloxacin	0.20	0.53	0.29	0.34

3. Conclusion

In the present work, a carboxyl functionalized quinoline derivative **L** was synthesized by Pfitzinger reaction. Four coordination complexes have been prepared based on **L** and structurally characterized which all show dinuclear structure. These complexes were assayed for their antibacterial (*B. subtilis* ATCC 6633, *E. coli* ATCC 35218, *P. aeruginosa* ATCC 27853 and *S. aureus* ATCC 6538) activities by MTT method. The results demonstrate that these new complexes showed antibacterial activities against selected bacterial. The results provide a promising foundation for the development of new metallodrugs with a broad spectrum of potential applications.

4. Experimental

4. 1. Chemistry

The IR spectra were taken on a Vector22 Bruker spectrophotometer (400–4000 cm^{-1}) with KBr pellets. 1H NMR spectra were measured on a Bruker AM 500 spectrometer. Chemical shifts were reported in ppm relative to Me4Si as internal standard. Elemental analyses for C, H and N were performed on a Perkin-Elmer 240 C analyzer. UV-visible spectra were measured on a Shimadzu UV-3600 spectrophotometer.

2-(4-bromophenyl)quinoline-4-carboxylic acid (L): A mixture of isatin (1.18 g, 8.00 mmol), 4-bromoacetophenone (0.40 g, 2.00 mmol) and potassium hydroxide (2.24 g, 40.00 mmol) in 2 mL of ethanol and 18 mL of water was refluxed for 12 h. Then the orange solution was cooled to room temperature and then poured into 20 mL of water. The solution was adjusted to pH 4 with 1 M HCl. The resulting brown precipitate was filtered, washed with water and dried in vacuo to give the product. Yield: 91%. IR (KBr, cm^{-1}): 3445, 2361, 1714, 1588, 1544, 1490, 1403, 1367, 1227, 1197, 1075, 1007, 831, 802, 766, 713, 541, 514. ^{1}H NMR (500 MHz, DMSO, δ): 8.65 (d, J = 8.0 Hz, 1H), 8.46 (s, 1H), 8.27 (d, J = 8.5 Hz, 2H), 8.17 (d, J = 8.0 Hz, 1H), 7.87 (t, 1H), 7.77 (d, J = 8.5 Hz, 2H), 7.21 (t, 1H). Anal. Calcd for $C_{16}H_{10}BrNO_2$: C, 58.56; H, 3.07; N, 4.27. Found: C, 58.67; H, 3.04; N, 4.29%.

4. 2. General Procedure for the Synthesis of Complexes 1–4.

2-phenylquinoline-4-carboxylic derivatives (0.04 mmol) in methanol solution (8 mL) was added to methanol solution (4 mL) of metal acetate (0.04 mmol), respectively. The resulting solution was left to stand at room temperature for a few days to give the corresponding block crystals suitable for X-ray diffraction analysis.

$[Mn_2(L)_4(CH_3OH)_4]$ (1) Yield: 66%, IR (KBr, cm^{-1}): 3440, 3061, 2361, 1639, 1587, 1403, 1322, 1072, 1029, 1005, 809, 760, 662, 466. Anal. Calcd for $C_{68}H_{52}Br_4N_4O_{12}Mn_2$: C, 52.81; H, 3.39; N, 3.62. Found: C, 52.96; H, 3.37; N, 3.63%.

$[Co_2(L)_4(CH_3OH)_4]$ (2) Yield: 45%, IR (KBr, cm^{-1}): 3446, 3065, 2361, 1645, 1603, 1536, 1464, 1404, 1367, 1032, 810, 759, 666, 468. Anal. Calcd for $C_{68}H_{52}Br_4N_4O_{12}Co_2$: C, 52.53; H, 3.37 N,3.60. Found: C, 52.69; H, 3.35; N, 3.62%.

$[Zn_2(L)_4(CH_3OH)_4]$ (3) Yield: 72%, IR (KBr, cm^{-1}): 3445, 3063, 2361, 1651, 1588, 1547, 1403, 1321, 1106, 1073, 1029, 810, 761, 665, 469. Anal. Calcd for $C_{68}H_{52}Br_4N_4O_{12}Zn_2$: C, 52.10; H, 3.34; N, 3.57. Found: C, 52.31; H, 3.32; N, 3.58%.

$[Cd_2(L)_4(CH_3OH)_4]$ (4) Yield: 68%, IR (KBr, cm^{-1}): 3445, 2361, 1586, 1542, 1486, 1400, 1316, 1103, 1072, 1010, 900, 808, 759, 663, 469. Anal. Calcd for $C_{68}H_{52}Br_4N_4O_{12}Cd_2$: C, 49.15; H, 3.15; N, 3.37. Found: C, 49.34; H, 3.13; N, 3.39%.

4. 3. *X*-ray Crystallography

The data were collected on a Bruker Smart Apex CCD diffractometer equipped with graphite-monochromated Mo K_α (λ = 0.71073 Å) radiation using a ω-2θ scan mode at 293 K. The collected data were reduced using the SAINT program,[27] and multi-scan absorption corrections were performed using the SADABS program.[28] The structures were solved by direct methods and refined against F^2 by full-matrix least-squares methods using the SHELXTL.[29] All non-hydrogen atoms were found in alternating difference Fourier syntheses and least-squares refinement cycles and, during the final cycles, refined anisotropically. All the hydrogen atoms were generated geometrically and reffned isotropically using the riding model except the hydrogen atoms of methanol molecules, which were located directly from the Fourier map.

4. 4. Bioassay Conditions

The antibacterial activity of the synthesized compounds was tested against *B. subtilis, E. coli, P. aeruginosa* and *S. aureus* using MH medium (Mueller-Hinton medium: casein hydrolysate 17.5 g, soluble starch 1.5 g, beef extract 1000 mL). The IC_{50} (half minimum inhibitory concentrations) of the test compounds were determined by a colorimetric method using the dye MTT (3-(4,5-dimethylth-iazol-2-yl)-2,5-diphenyl tetrazolium bromide). A stock solution of the synthesized compound (100 μg/mL) in DMSO was prepared and graded quantities of the test compounds were incorporated in specified quantity of sterilized liquid MH medium. A specified quantity

of the medium containing the compound was poured into microtitration plates. Suspension of the microorganism was prepared to contain approximately 10^5 cfu/mL and applied to microtitration plates with serially diluted compounds in DMSO to be tested and incubated at 37 °C for 24 h. After the MICs were visually determined on each of the microtitration plates, 50 μL of PBS (phosphate buffered saline 0.01 mol/L, pH 7.4, $Na_2HPO_4 \cdot 12H_2O$ 2.9 g, KH_2PO_4 0.2 g, NaCl 8.0 g, KCl 0.2 g, distilled water 1000 mL) containing 2 mg of MTT/mL was added to each well. Incubation was continued at room temperature for 4–5 h. The content of each well was removed, and 100 μL of isopropanol containing 5% 1 mol/L HCl was added to extract the dye. After 12 h of incubation at room temperature, the optical density (OD) was measured with a microplate reader at 550 nm.

5. Supplementary Information

CCDC 976246 (**1**), 976247 (**2**), 976248 (**3**), and 976249 (**4**) contain the supplementary crystallographic data for this paper. These data can be obtained free of charge at http://www.ccdc.cam.ac.uk/const/retrieving.html or from the Cambridge Crystallographic Data Centre (CCDC), 12 Union Road, Cambridge CB2 1EZ, UK; fax: +44(0)1223-336033 or e-mail: deposit@ccdc.cam.ac.uk.

6. Acknowledgments

This work was supported by the National Natural Science Foundation of China (21301108).

7. References

1. B. Rosenberg, L. V. Camp, T. Krigas, *Nature* **1965**, *205*, 698.
2. (a) I. Kostova, *Curr. Med. Chem.* **2006**, *13*, 1085–1107; (b) C. G. Hartinger, A. A. Nazarov, S. M. Ashraf, P. J. Dyson, B. K Keppler, *Curr. Med. Chem.* **2008**, *15*, 2574–2591.
3. D. R. Richardson, D. S. Kalinowski, V. Richardson, P. C. Sharpe, D. B. Lovejoy, M. Isalam, P. V. Bernhardt, *J. Med. Chem.* **2009**, *52*, 1459–1470.
4. M. X. Li, L. Z. Zhang, M. Yang, J. Y. Niu, J. Zhou, *Bioorg. Med. Chem.* **2012**, *22*, 2418–2423.
5. Z. F. Chen, Y. F. Shi, Y. C. Liu, X. Hong, B. Geng, Y. Peng, H. Liang, *Inorg. Chem.* **2012**, *51*, 1998–2009.
6. D. Santos, B. Parajón-Costa, M. Rossi, F. Caruso, D. Benítez, J. Varela, H. Cerecetto. M. González, N. Gómez, M. E. Caputto, A. G. Moglioni, G. Y. Moltrasio, L. M. Finkielsztein, D. Gambino, *J. Inorg. Biochem.* **2012**, *117*, 270–276.
7. R. Mehrotra, S. N. Shukla, P. Gaur, A. Dubey, *Eur. J. Med. Chem.* **2012**, *50*, 149–153.
8. M. Patra, G. Gasser, N. Metzler-Nolte, *Dalton Trans.* **2012**, *41*, 6350–6358.
9. I. Turel, *Coord. Chem. Rev.* **2002**, *232*, 27–47.
10. A. Tanitame, Y. Oyamada, K. Ofuji, M. Fujimoto, N. Iwai, Y. Hiyama, K. Suzuki, H. Ito, H. Terauchi, M. Kawasaki, K. Nagai, M. Wachi, J. Yamagishi, *J. Med. Chem* **2004**, *47*, 3693–3696.
11. B. R Short, M. A Vargas, J. C Thomas, S. O'Hanlon, M. C. Enright, *J. Antimicrob. Chemother.* **2006**, *57*, 104–109.
12. V. Prachayasittikul, S. Prachayasittikul, S. Ruchirawat, V. Prachayasittikul, *Drug Des. Devel. Ther.* **2013**, *7*, 1157–1178.
13. S. Manohar, U. C. Rajesh, S. I. Khan, B. L. Tekwani, D. S. Rawat, *Med. Chem. Lett.* **2012**, *3*, 555–559.
14. A. M. L. Carmo, F. M. C. Silva, P. A. Machado, A. P. S. Fontes, F. R. Pavan, C. Q. F. Leite, S. R. de A. Leite, E. S. Coimbra, A. D. Da Silva, *Biomed. Pharmacother.* **2011**, *65*, 204–209.
15. E. K. Efthimiadou, Y. Sanakis, C. P. Raptopoulou, A. Karaliota, N. Katsaros, G. Psomas, *Bioorg. Med. Chem. Lett.* **2006**, *16*, 3864–3867.
16. Q. D. Zhou, T. W. Hambley, B. J. Kennedy, P. A. Lay, P. Turner, B. Warwick, J. R. Biffin, H. L. Regtop, *Inorg. Chem.* **2000**, *39*, 3742–3748.
17. X. H. Bu, M. L. Tong, Y. B. Xie, J. R. Li, H. C. Chang, S. Kitagawa, J. Ribas, *Inorg. Chem.* **2005**, *44*, 9837–9846.
18. F. P. Pruchnik, M. Bańbuła, Z. Ciunik, M. Latocha, B. Skop, T. Wilczok, *Inorg. Chim. Acta* **2003**, *356*, 62–68.
19. J. Kubo, J. R. Lee, I. Kubo, *J. Agric. Food Chem.* **1999**, *47*, 533–537.
20. S. S. M. Hassan, R. M. El-Bahnasawv, N. M. Rizk, *Anal. Chim. Acta* **1997**, *351*, 91–96.
21. W. J. Mao, P. C. Lv, L. Shi, H. Q. Li, H. L. Zhu, *Bioorg. Med. Chem.* **2009**, *17*, 7531–7536.
22. S. C. Chen, Z. H Zhang, Q. Chen, L. Q. Wang, J. Xu, M. Y. He, M. Du, X. P. Yang, R. A. Jones, *Chem. Commum.* **2013**, *49*, 1270–1272.
23. A. Tarushi, G. Psomas, C. P. Raptopoulou, D. P. Kessissoglou, *J. Inorg. Biochem.* **2009**, *103*, 898–905.
24. (a) W. Pfitzinger, *J. Prakt. Chem.* **1897**, *56*, 283-320; (b) M. G. A. Shvekhgeimer, *Chem. Heterocycl. Com.* **2004**, *40*, 257–294; (c) H. Zhu, R. F. Yang, L. H. Yun, J. Li, *Chin. Chem. Lett.* **2010**, *21*, 35–38.
25. F. Y. Yi, J. Zhang, H. X. Zhang, Z. M. Sun, *Chem. Commun.* **2012**, *48*, 10419–10421.
26. T. Allman, R. C. Goel, N. K. Jha, A. L. Beauchamp, *Inorg. Chem.* **1984**, *23*, 914–918.
27. Bruker, SMART and SAINT. Bruker AXS Inc., Madison, Wisconsin, USA, **2002**.
28. G. M. Sheldrick, SADABS. Program for Empirical Absorption Correction of Area Detector, University of Göttingen, Germany, **1996**.
29. G. M. Sheldrick, *Acta Crystallogr.* **2008**, *A64*, 112–122.

Povzetek

Serija dvojedrnih koordinacijskih spojin prehodnih elementov s strukturo mlinskega kolesa z derivatom 2-fenilkinolin-4-karboksilatnega liganda **L** je bila sintetizirana in okarakterizirana z IR, elementno analizo in rentgensko monokristalno analizo. Biološka aktivnost liganda in njegovih kompleksov je bila določena s testiranjem antibakterijske aktivnosti na *Escherichia coli, Pseudomonas aeruginosa*, *Bacillus subtilis* in *Staphylococcus aureus*. Rezultati so pokazali, da imajo kompleksi večjo aktivnost kot prosti ligand ali enostavne anorganske soli teh prehodnih elementov. Največjo aktivnost proti *Staphylococcus aureus* imata Zn(II) in Cd(II) kompleks z IC_{50} 0.57 μg/mL oziroma 0.51 μg/mL.

Electronic Supplementary Information for

Synthesis, Crystal Structures, and Antibacterial Evaluation of Metal Complexes Based on Functionalized 2-phenylquinoline Derivatives

Jie Qin[1]*, [2] Fu-Xiang Li,[1] Le Xue,[1] Na Lei,[1] Qing-Ling Ren,[1] Dan-Yang Wang[1] and Hai-Liang Zhu[1]

[1] *School of Life Sciences, Shandong University of Technology, Zibo, China*

[2] *State Key Laboratory of Coordination Chemistry, School of Chemistry and Chemical Engineering, Nanjing University, Nanjing, China*

* *Corresponding author: E-mail: qinjietutu@163.com*

Received: 17-12-2013

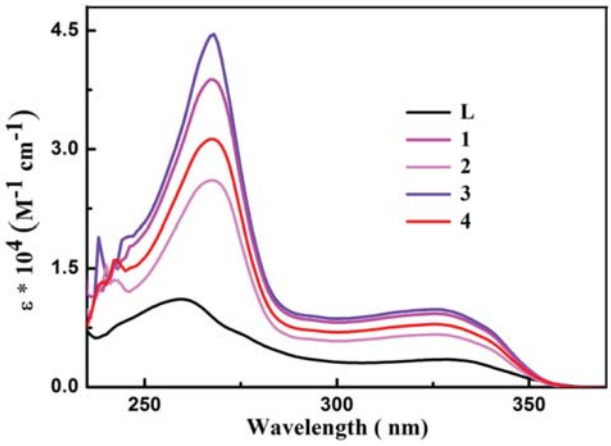

Figure S1. Absorption spectra of ligand **L** and complexes **1**–**4** in DMSO/H_2O (1:1, v/v).

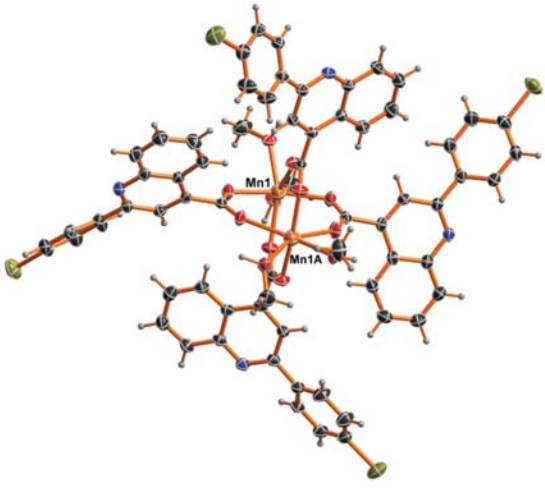

Figure S2. ORTEP view of **1** at the 50% probability level.

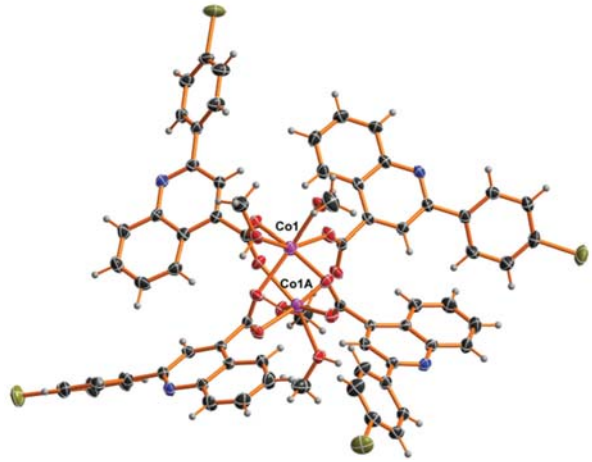

Figure S3. ORTEP view of **2** at the 50% probability level.

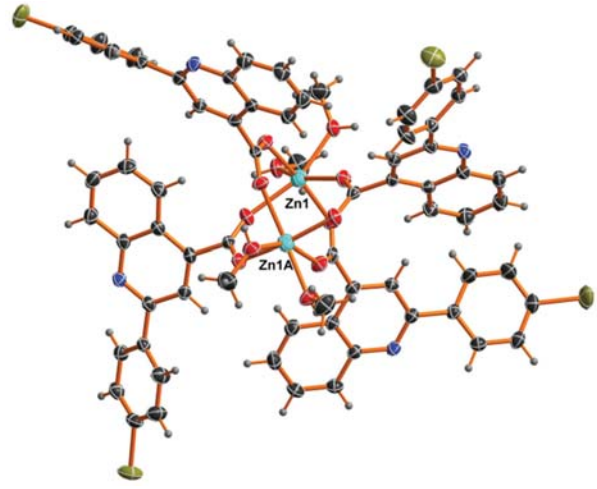

Figure S4. ORTEP view of **3** at the 50% probability level.

Table S1. Selected Bond Distance (Å) and Angles (deg) for **1**.

Mn(1)-O(1)	2.247(2)	Mn(1)-O(2)	2.129(2)
Mn(1)-O(3)	2.219(2)	Br(1)-C(3)	1.899(3)
C(16)-O(1)	1.241(4)	C(16)-O(2)$^{\#2}$	1.257(4)
O(2)$^{\#1}$-Mn(1)-O(2)	166.22(2)	O(2)$^{\#1}$-Mn(1)-O(3)	103.86(8)
O(2)-Mn(1)-O(3)	86.82(8)	O(3)-Mn(1)-O(3)$^{\#1}$	79.69(1)
O(2)$^{\#1}$-Mn(1)-O(1)$^{\#1}$	90.39(8)	O(2)-Mn(1)-O(1)$^{\#1}$	83.23(8)
O(3)-Mn(1)-O(1)$^{\#1}$	153.82(8)	O(3)$^{\#1}$-Mn(1)-O(1)$^{\#1}$	79.30(8)
O(1)$^{\#1}$-Mn(1)-O(1)	124.77(2)	O(1)-C(16)-O(2)$^{\#2}$	126.7(3)

Symmetry transformations used to generate equivalent atoms:
#1 –x+2, –y+3/2, z; #2 y+1/4, –x+7/4, –z+7/4; #3 –y+7/4, x–1/4, –z+7/4

Table S2. Selected Bond Distance (Å) and Angles (deg) for **2**.

Co(1)-O(1)	2.196(2)	Co(1)-O(2)$^{\#1}$	2.036(2)
Co(1)-O(3)	2.146(2)	Br(1)-C(3)	1.896(3)
C(5)-C(6)	1.299(4)	C(7)-C(8)	1.378(5)
C(16)-O(1)	1.238(4)	C(16)-O(2)	1.258(4)
O(2)$^{\#1}$-Co(1)-O(2)$^{\#2}$	167.19(2)	O(2)$^{\#1}$-Co(1)-O(3)$^{\#3}$	102.25(8)
O(2)$^{\#2}$-Co(1)-O(3)$^{\#3}$	87.57(9)	O(3)$^{\#3}$-Co(1)-O(3)	80.87(1)
O(2)$^{\#1}$-Co(1)-O(1)$^{\#3}$	89.83(8)	O(2)$^{\#2}$-Co(1)-O(1)$^{\#3}$	84.19(8)
O(3)$^{\#3}$-Co(1)-O(1)$^{\#3}$	155.56(8)	O(3)-Co(1)-O(1)$^{\#3}$	78.47(8)
O(2)$^{\#1}$-Co(1)-O(1)	84.19(8)	O(1)$^{\#3}$-Co(1)-O(1)	124.35(1)

Symmetry transformations used to generate equivalent atoms:
#1 –y+3/4,x–1/4, –z+7/4; #2 y+1/4, –x+3/4, –z+7/4; #3 –x+1, –y+1/2, z

Table S3. Selected Bond Distance (Å) and Angles (deg) for **3**.

Zn(1)-O(1)	2.2159(8)	Zn(1)-O(2)$^{\#1}$	2.0210(8)
Zn(1)-O(3)$^{\#3}$	2.1551(9)	Br(1)-C(3)	1.897(3)
C(16)-O(1)	1.238(3)	C(16)-O(2)	1.264(3)
O(2)$^{\#1}$-Zn(1)-O(2)$^{\#2}$	167.68(1)	O(2)$^{\#1}$-Zn(1)-O(3)$^{\#3}$	101.58(8)
O(2)$^{\#2}$-Zn(1)-O(3)$^{\#3}$	87.91(8)	O(2)$^{\#2}$-Zn(1)-O(3)	101.58(8)
O(3)$^{\#3}$-Zn(1)-O(3)	80.22(1)	O(2)$^{\#1}$-Zn(1)-O(1)	84.27(8)
O(2)$^{\#2}$-Zn(1)-O(1)	89.91(8)	O(3)$^{\#3}$-Zn(1)-O(1)	79.07(7)
O(3)-Zn(1)-O(1)	155.88(7)	O(1)-Zn(1)-O(1)$^{\#3}$	123.58(1)

Symmetry transformations used to generate equivalent atoms:
#1 –y+3/4, x–1/4, –z+7/4; #2 y+1/4, –x+3/4, –z+7/4; #3 –x+1, –y+1/2, z